IEEE Access
Multidisciplinary | Rapid Review | Open Access Journal

Received June 3, 2019, accepted June 11, 2019, date of publication June 17, 2019, date of current version July 1, 2019.

Digital Object Identifier 10.1109/ACCESS.2019.2923358

A Model-Free Control Method for Synchronous Vibration of Active Magnetic Bearing Rotor System

YANGBO ZHENG, NI MO, YAN ZHOU, AND ZHENGANG SHI
Institute of Nuclear and New Energy Technology of Tsinghua University, Beijing 100084, China
Collaborative Innovation Center of Advanced Nuclear Energy Technology, Beijing 100084, China
The Key Laboratory of Advanced Reactor Engineering and Safety, Ministry of Education, Beijing 100084, China

Corresponding author: Zhengang Shi (shizg@tsinghua.edu.cn)

This work was supported by the National Science and Technology Major Project of China under Grant 2019ZX06903019.

ABSTRACT The unbalanced force on the active magnetic bearing (AMB) rotor system is the main reason of system vibrations, which always have periodic repetitive characteristics. However, the closed-loop feedback control system (CFCS) is difficult to achieve effective control of these repetitive problems. In this paper, we firstly analyzed the synchronous vibration by taking AMB rotor mass imbalance as an example. Then, we proposed a model-free control (MFC) method based on the Newton-type ILC algorithm, and the key of this MFC is to use a partial derivative (P-D) of the output with respect to the input. The simplicity of this algorithm lies in that and the P-D is calculated by only using the input and output (I/O) data of the system and then used to adjust the ILC gain. Subsequently, we proposed a parallel plug-in control scheme based on existing AMB control system to suppress synchronous vibration. Finally, we carried out the simulation and experiment to research the control method mentioned in this paper. The results show that the MFC has a good control effect on AMB synchronous vibration. Notably, this MFC for synchronous vibration has the advantages of being without system model, simple design and good portability, and can provide theoretical and experimental basis for the application of AMB in high precision and high speed fields.

INDEX TERMS Active magnetic bearing, synchronous vibration, model-free, iterative learning control parallel control scheme.

I. INTRODUCTION

Many traditional mechanical bearings are difficult to meet requirements of some occasions due to mechanical friction, serious wear, and lubrication, etc. Fortunately, AMB has many advantages, such as no mechanical contact, no wear, and no lubrication, etc., can effectively avoid the problems existing in traditional mechanical bearings [1]. Moreover, AMB has been verified in the field of high speed, high precision and high clean occasions, such as the primary helium circulator and helium compressor used in primary helium circulation system of high temperature gas-cooled reactor [2], [3], and high speed motor [4]. But due to limited precision of processing, manufacturing and defects of materials, etc., which may lead the rotor mass imbalance. Meanwhile, imprecision of installation and debugging always lead to misalignment of the geometric centers between the stator and the rotor. Additionally, rotor distortion and residual objects attached to the rotor that may occur during operation. All of these reasons would lead to complex unbalanced problems of AMB rotor system eventually. From [5]–[8], the unbalanced force on AMB rotor system is the main reason of synchronous vibration and multi-frequency vibration in rotating machinery equipped with AMB. Furthermore, the unbalance problems would become more complex and more serious as the rotating machinery is operating, and even threaten the safety and reliability of the system.

In AMB control system, CFCS is necessary. There are many research fruits in the field of unmolded dynamics and actuator faults and unknown output of the control system [9]–[11], iterative feedback tuning [12], [13]. Furthermore, besides conventional PID controller, 2- degree of

The associate editor coordinating the review of this manuscript and approving it for publication was Salman Ahmed.

freedom (DOF) controller, nonlinear smooth feedback control method and linear parameter varying controller were studied for AMB [14]–[16]. But these feedback control methods were designed for the stability of the system, not for periodic vibrations produced by rotor imbalance.

There are many unbalanced control methods for AMB rotor system, such as the traditional mechanical balance compensation method, which is commonly used before installation, but it may unsuitable to tackle unbalance found after installation or occurred in the operation. Fortunately, due to the active control characteristics of AMB [1], [17],the vibrations can be suppressed by the control method when the rotor is suspended by AMB. In [18], the unbalance control technologies of AMB system are comprehensively summarized, and divided into two categories, including force freedom and force control respectively. From the literature investigation, most of current AMB rotor unbalance control algorithms rely heavily on the rotor system model [19]–[21], and some control algorithms can only be effective at the fixed speed. Furthermore, most of the control methods just verified on the simulation platform, but not fully verified on the actual AMB system [19]–[23].

More significantly, AMB is a multi-input and multi-output nonlinear system with strong coupling, time-varying and structural uncertainty. In the design of CFCS, Taylor linearization is always carried out at the equilibrium point. But the controller in CFCS (always PID controller) without learning from previous system formation has little effect on periodic vibration control [1], [17].

Fortunately, as one of data-driven control method, ILC can deal with repetitive problems as the periodic vibration stated in this paper by using the previous system information, and need little system model [24], which provides the foundation for the MFC applied to suppress AMB synchronous vibration researched in this paper. Recently, many application problems have been solved, such as input constraint [25], [26], data dropout and so on [27]–[29]. Furthermore, ILC has been successfully used to suppress periodic disturbance of linear motor and microscale and nanoscale tracking systems [30], [31].

To sum up, the purpose of this paper is mainly to put forward and achieve a completely MFC method based on Newton-type ILC for synchronous vibration of AMB rotor system with the advantages of ILC over repetitive problems and needing little system model information. And his paper is arranged as follows: Section II analyzes the periodic vibration by taking AMB rotor mass imbalance as an example. In Section III, the MFC method based on Newton-type ILC is proposed and analyzed in detail. In Section IV, the parallel plug-in control scheme is designed to achieve the MFC method based on the existing AMB CFCS. In Section V, simulations and experiments are carried out to verify the effectiveness of the methods, and the results are discussed here. Finally, some conclusions, future directions and works have been summarized in Section VI.

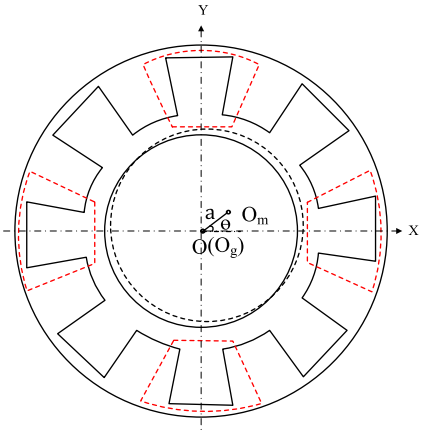

FIGURE 1. The schematic diagram of rotor mass imbalance model in the axial section.

II. AMB ROTOR SYNCHRONOUS VIBRATION MECHANISM ANALYSIS

There are many factors that can produce periodic vibrations of rotating machinery, but the most important one is the synchronous vibration caused by the rotor mass imbalance [32]. Here, we take it as an example to analyze the mathematical mechanism. Certainly, other periodic vibrations caused by corrosion, cracks or residues can be equivalent to the rotor mass imbalance. In this paper, the synchronous vibration generated by the rotor mass imbalance is analyzed by the theory of mechanical system vibration [33]. The rotor mass imbalanced model in the axial section is shown in Fig.1.
where O(0, 0) is the geometric center of the stator, and the fixed rectangular coordinate system OXY is established with this point as the origin of coordinates, and O_g is the geometric center of the rotor. Here we assume that there is no geometric eccentricity, that is, the rotor geometric center overlaps with the stator geometric center. In addition, $O_m(x_m, y_m)$ is the rotor mass center, $O_gO_m = a$ is the mass eccentricity, ω is the rotor rotational speed and θ is the initial phase of the mass center with respect to OXY. Thus, the geometrical relationship can be expressed as

$$\begin{cases} x_m = a\cos\theta \\ y_m = a\sin\theta \end{cases} \tag{1}$$

When the rotor is running with speed ω, the components of the unbalanced centrifugal force in the X and Y directions can be calculated as

$$\begin{cases} f_{mx} = m\omega^2 a\cos(\omega t + \theta) \\ f_{my} = m\omega^2 a\sin(\omega t + \theta) \end{cases} \tag{2}$$

Since a rigid rotor used in the AMB experimental system has typical second-order characteristics, the differential equations for the radial vibration of the rotor system can be written as

$$\begin{cases} m\ddot{x} + c\dot{x} + kx = m\omega^2 a\cos(\omega t + \theta) \\ m\ddot{y} + c\dot{y} + ky = m\omega^2 a\sin(\omega t + \theta) \end{cases} \tag{3}$$

where c is rotor damping and k is rotor stiffness. The solution of the equations (3) can be expressed as

$$\begin{cases} x(t) = C_{1x}e^{x_1 t} + C_{2x}e^{x_2 t} + C_{mx}\cos(\omega t + \varphi_x) \\ y(t) = C_{1y}e^{y_1 t} + C_{2y}e^{y_2 t} + C_{my}\sin(\omega t + \varphi_y) \end{cases} \tag{4}$$

where x_1, x_2, y_1 and y_2 are the eigenvalues, C_{1x}, C_{2x}, C_{mx}, C_{1y}, C_{2y}, C_{my}, φ_x and φ_y are constants of the solution of equations (3). Since the AMB rotor system is stable based on CFCS, the eigenvalues are located in the left half complex plane. This means the exponential terms ($C_{1x}e^{x_1 t} + C_{2x}e^{x_2 t}$ and $C_{1y}e^{y_1 t} + C_{2y}e^{y_2 t}$) of equations (4) will decay over time, and the rest components of the motion are the rotor vibrations and can be expressed as

$$\begin{cases} x(t) = C_{mx}\cos(\omega t + \varphi_x) \\ y(t) = C_{my}\sin(\omega t + \varphi_y) \end{cases} \tag{5}$$

As described in equations (5), the unbalanced centrifugal force caused by rotor mass imbalance eventually leads to the simple harmonic vibration with the same frequency as ω in the X and Y directions. Additionally, other multi-frequency vibrations will occur due to misalignment of the stator and the rotor [34], sensor runout, etc., which will not be analyzed in detail here.

The simple harmonic vibration of the rotor described in equations (5) is essentially the AMB rotor synchronous vibration, which is one of the most difficult problems to be solved for rotating machinery equipped with AMB. In severe cases, it will lead to deterioration of system performance, shortening of service life, and even threatening of system safety.

More seriously, if the vibration amplitude is too large in AMB, the rotor and the catcher bearing would be initially rubbed, which would cause irreparable damage to the system structure. Fortunately, AMB can provide the active control ability for the rotor, and the traditional bearings cannot be comparable in this aspect [17].

From the description above, due to the complex and variable operating conditions of the AMB system, structural uncertainties, the system vibration mechanism is complex. So the traditional control methods based on model are difficult to apply to the AMB rotor system vibration control.

III. MODEL-FREE CONTROL METHOD

A. INTRODUCTION TO THE BASIC AGORITHM

The MFC method proposed in this paper is based on the iterative learning algorithm, which can achieve effective control of repetitive problems with little system model information. And it was used to control repetitive tasks of robots and established under a strong engineering application background [35].

Since most of the controlled plants in the industry have nonlinear characteristics, and for the sake of coinciding with the AMB with single DOF, iterative learning algorithm is described by taking a discrete time-varying single input single output (SISO) system as an example. The system is described as

$$\begin{cases} x_k(t+1) = f(x_k(t), u_k(t)) \\ y_k(t) = g(x_k(t)) \end{cases} \quad x_k(0) = x_0 \tag{6}$$

where $t = [0, 1, 2, \cdots, N-1]$, N is the iterative learning step size, k$\epsilon\{0, 1, 2, \cdots\}$ is the iterative index, $x_k(t) \in R^n$ (n is the system state dimension), $y_k(t) \in R$ and $u_k(t) \in R$ are the state vector, the output and the input, respectively. $f(\cdot)$ and $g(\cdot)$ are the state vector function with n dimensional and the smooth output function. Meanwhile, we assume the system has identical initial conditions for each iteration. The goal of ILC is to find the target control sequence $u_d(t)$ through repetitive iterations, so that the actual output sequence $y_k(t)$ can track the target output sequence $y_d(t)$. The general control output can be expressed as

$$u_{k+1}(t) = \mathcal{F}(u_0(t), \cdots, u_k(t), e_0(t), \cdots, e_k(t), e_{k+1}(t)) \tag{7}$$

where $e_k(t) = y_d(t) - y_k(t)$. According to equation (7), the current control output is a linear or non-linear combination of past control outputs, past control errors and current control error. So it is a control method with memory function and belongs to intelligent control [36].

B. ITERAIVE LEARNING CONTROL BASED ON NEWTON METHOD

If the controlled plant is a linear time-invariant system, and the system model is known or can be easily identified, the ILC algorithm design is very simple, such as P-ILC, PD-ILC, PID-ILC, and other compound control methods based on ILC [36]–[41]. However, due to the nonlinearity and strong coupling, and the complex unbalance problems of the AMB rotor system, accurate model is almost impossible obtained. Therefore, the classical ILC algorithms are difficult to apply to suppress the synchronous vibration of AMB rotor system.

Here, this paper proposes the MFC method with P-D calculated by using the system I/O data in the basis of Newton-type ILC scheme, which is based on the Newton method [42], [43] or the Quasi-Newton method [44], [45]. For further analysis of the algorithm, the difference equation of the plant described in equations (6) are rewrote as algebraic equations. Firstly, the sequences of $u_k(t)$, $y_k(t)$ and $e_k(t)$ are defined as

$$\begin{cases} u_k(t) = [u_k(0), u_k(1), \cdots, u_k(N-1)]^T \\ y_k(t) = [y_k(1), y_k(2), \cdots, y_k(N)]^T \\ e_k(t) = [y_d(1) - y_k(1), y_d(2) - y_k(2), \\ \cdots, y_d(N) - y_k(N)]^T \end{cases} \tag{8}$$

According to the difference equations (6), the input control sequence $u_k(t)$ and the output sequence $y_k(t)$ satisfy the following relations as expressed in equations (9) and

equation (10).

$$\begin{cases} y_k(1) = g\{x_k(1)\} = g\{f(x_k(0), u_k(0))\} \\ = \mathcal{H}_1\{x_k(0), u_k(0)\} \\ y_k(2) = g\{x_k(2)\} = g\{f(x_k(1), u_k(1))\} \\ = \mathcal{H}_2\{x_k(0), u_k(0), x_k(1), u_k(1)\} \\ \vdots \\ y_k(N) = g\{x_k(N)\} = g\{f(x_k(N-1), u_k(N-1))\} \\ = \mathcal{H}_N\{x_k(0), u_k(0), \cdots, x_k(N-1), u_k(N-1)\} \end{cases} \tag{9}$$

Furthermore, the differential equations (9) can be described as the algebraic equation.

$$y_k(t) = \mathcal{H}(u_k(t)) \tag{10}$$

where $\mathcal{H}(.)$ is a compound function of $f(.)$ and $g(.)$. Now we assume that the system can be reachable, that is, there exists a unique target input sequence $u_d(t)$ for the target output sequence $y_d(t)$. Therefore, the execution of the ILC algorithm is transformed into the solution of the algebraic equation (10). According to Newton method [42], the Newton-type ILC algorithm can be written as

$$u_{k+1}(t) = u_k(t) + [\frac{\partial \mathcal{H}(u_k(t))}{\partial u_k(t)}]^{-1} e_k(t) \tag{11}$$

Mathematically, $\frac{\partial \mathcal{H}(u_k(t))}{\partial u_k(t)}$ is a dynamic linearization method for the controlled plant described as equations (6). Moreover, the ILC algorithm described in equation (11) based on Newton method has quadratic convergence characteristics. Namely,

$$\|u_{k+1}(t) - u_d(t)\| \leq \gamma \|u_k(t) - u_d(t)\|^2, \quad \gamma \in (0, 1) \tag{12}$$

Therefore, the key of the ILC algorithm based on Newton method becomes how to calculate $[\frac{\partial \mathcal{H}(u_k(t))}{\partial u_k(t)}]^{-1}$. Some theoretical methods are researched in [42]–[45], but they are very complicated, and difficult to avoid the analysis of the controlled plant model and complex operation of the matrix inversion. Moreover, singular Jacobian matrix problems may occur here. So this paper proposes a simple and approximate calculation method to avoid the problems stated above. And this method does not need the system model information and is equivalent with matrix inversion in SISO system.

C. ITERAIVE LEARNING GAIN ESTIMATION

As the MFC for synchronous vibration proposed in this paper is based on the existing AMB CFCS, the system has already worked near the equilibrium point. That is to say, the system has well certain linearization basis. Therefore, calculating the system P-D in each iteration, is essentially equivalent to solve the parameter $\varphi_k(t)$ of the following linear equation.

$$\Delta y_k(t+1) = \varphi_k(t) \Delta u_k(t) \tag{13}$$

where $\Delta y_k(t+1) = y_k(t+1) - y_k(t)$ and $\Delta u_k(t) = u_k(t) - u_k(t-1)$. Combining with equations (11) and (13), it can be seen that $\varphi_k(t) = \frac{\partial \mathcal{H}(u_k(t))}{\partial u_k(t)}$. In other words, through the transformation of the algorithm, the nonlinear problem has been transformed into a serious of dynamic linearization problems. In order to estimate $\varphi_k(t)$, we first establish the following criterion function as expressed in equation (14) with reference to affine projection algorithm [46], dynamic linearization methods [46] and other MFC theory [48].

$$J(\varphi_k(t)) = \left|\Delta y_k(t) - \widehat{\Delta y_k}(t)\right|^2 + \lambda |\varphi_k(t) - \varphi_k(t-1)|^2 \tag{14}$$

where $\widehat{\Delta y_k}(t) = \varphi_{k-1}(t) \Delta u_{k-1}(t)$. Substituting equation (13) into equation (14), we can get

$$\begin{aligned} &J(\varphi_k(t)) \\ &= |y_k(t) - y_k(t-1) - \varphi_k(t)(u_k(t-1) - u_k(t-2))|^2 \\ &\quad + \lambda |\varphi_k(t) - \varphi_k(t-1)|^2 \end{aligned} \tag{15}$$

where $|y_k(t) - y_k(t-1) - \varphi_k(t)(u_k(t-1) - u_k(t-2))|^2$ is used to restrict the system control error, and $\lambda |\varphi_k(t) - \varphi_k(t-)|^2$ is used to limit the change rate of $\varphi_k(t)$. Here $\varphi_k(t)$ would not have great change because it is determined by the current system equilibrium point. $\lambda > 0$, is just a control factor, and does not affect the optimum solution. Then we solve the optimal solution of the criterion function as expressed in equation (15), and $\varphi_k(t)$ can be calculated as

$$\begin{aligned} &\varphi_k(t) \\ &= \varphi_k(t-1) + \frac{u_k(t-1) - u_k(t-2)}{\lambda + (u_k(t-1) - u_k(t-2))^2} \\ &\quad \times (y_k(t) - y_k(t-1) - \varphi_k(t-1)(u_k(t-1) - u_k(t-2))) \end{aligned} \tag{16}$$

Equation (16) is an equivalent calculation of the system P-D, and $\varphi_k(t)$ is a sign-invariant and bounded variable in the actual system. The P-D of AMB system is always a positive bounded variable, so it can be described as

$$\varphi_k(t) \in [\alpha, \beta] \tag{17}$$

where $\alpha = min\{\varphi_k(t)\}$ and $\beta = max\{\varphi_k(t)\}$. In order to ensure the convergence of the system control error, combining with equations (11) and (17), the range of ILC algorithm gain can be express as

$$[\frac{\partial \mathcal{H}(u_k(t))}{\partial u_k(t)}]^{-1} \in [0, \frac{1}{\beta}] \tag{18}$$

Therefore, $\varphi_k(t)$ with the same dimension as the iterative learning step N in each iteration can be calculated, and then used to set ILC algorithm gain with reference to equations (17) and (18).

D. MODEL-FREE CONTROL METHOD SYNNTHESIS

Through the above analysis, the iterative learning algorithm based on Newton method designed in this paper does not need any system model information. It only needs the system I/O data to calculate the P-D, which provides the parameter self-learning function for the Newton-type ILC. Of course, this

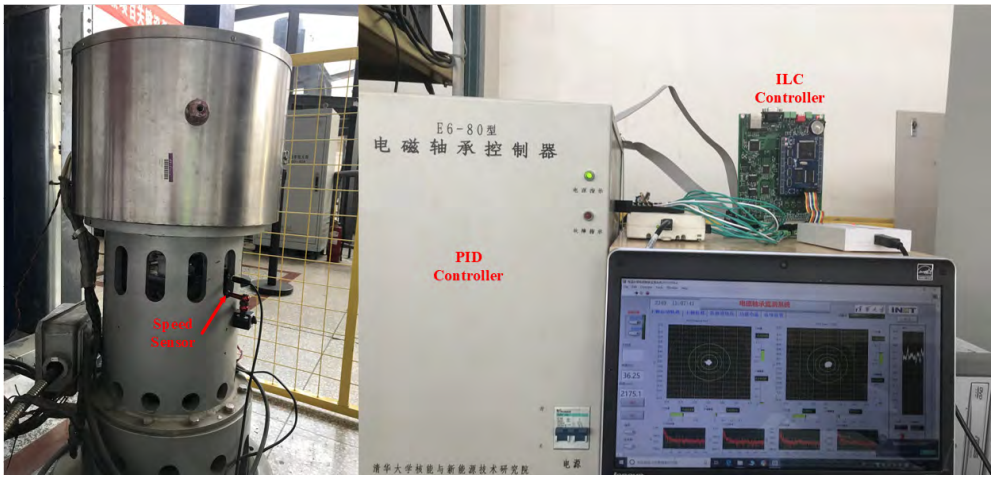

FIGURE 2. The AMB experimental system.

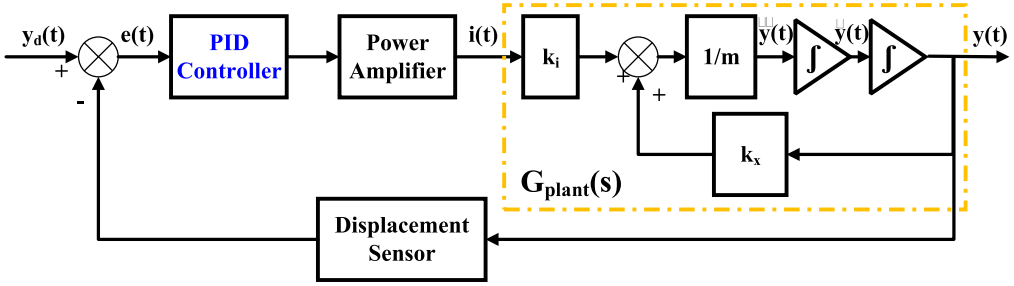

FIGURE 3. The AMB CFCS with single DOF.

MFC method is only suitable for discrete SISO control systems. Fortunately, AMB is always controlled by a distributed scheme in the digital control system, so MFC proposed in this paper can be used to suppress synchronous vibration of AMB rotor system. Here, the basic process of the MFC is summarized as follows:

Step 1: The control factor λ and the initial P-D ($\varphi_0(t)$) should be determined firstly. In order to avoid the non-convergence of the system control error, it can be obtained from equations (11), (17) and (18) that the initial learning gain cannot be too large, so the $\varphi_0(t)$ cannot be set too small.

Step 2: The system begins to learn, calculate and store $u_k(t)$, $y_k(t)$, $e_k(t)$ and $\varphi_k(t)$. When current iteration ends, it needs to check whether $e_k(t)$ meets the requirement or not. If the requirement is met, it means that $u_k(t)$ of the current iteration is the target control sequence $u_d(t)$, otherwise, it proceeds to Step 3.

Step 3: According to the $u_k(t)$, $e_k(t)$ and $\varphi_k(t)$ obtained in Step 2, the control input sequence $u_{k+1}(t)$ should be calculated according to equation (11). Then the variables would be renewed as the $u_{k+1}(t)$ inputted the system. This control process is executed repetitively until the system output $y_k(t)$ completely tracks $y_d(t)$.

IV. CONTROL SCHEME ANALYSIS

Equations (11), (16), (17) and (18) show that the control algorithm designed in this paper is a model-free open-loop proportional variable gain ILC algorithm. And it is used to suppress the AMB rotor synchronous vibration produced by unbalanced force mentioned in Section II.

A. CONTROL PLANT DESCRIPTION

The AMB system used in this paper is vertically arranged, as shown in Fig.2. And the CFCS is implemented based on PID controller.

As shown in Fig.2, the gravity of the AMB rotor is balanced by the axial thrust bearing. The upper and lower radial AMBs are used to achieve the stability control for four radial DOFs.

From the analysis of Section II, the unbalanced force mainly exists in the radial directions of the AMB rotor system. In order to facilitate the design of the control system, a distributed control scheme is adopted for the synchronous vibration in four radial directions. And the AMB CFCS with single DOF is shown in Fig.3.

where k_i and k_x are the current coefficient and displacement coefficient of the AMB system respectively, which are two constants related to the structure and equilibrium point after linearization. Therefore, the transfer function of the AMB with single DOF can be expressed as

$$G_{plant}(s) = \frac{k_i}{ms^2 - k_x} \tag{19}$$

Obviously, it is an open-loop unstable system, so the CFCS is necessarily used to achieve stability control for the AMB system [1].

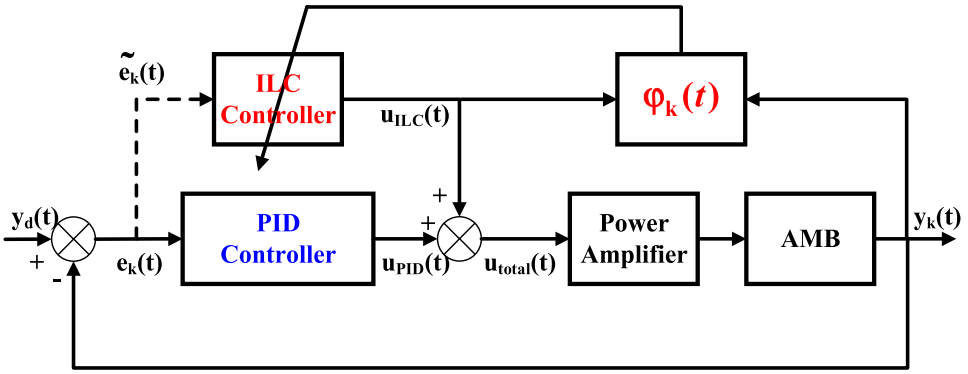

FIGURE 4. The parallel control scheme for AMB rotor synchronous vibration.

B. CONTROL SCHEME DESIGN

The synchronous vibration of AMB rotor system in this paper adopts a "on demand" strategy, which means it is used in plug-in mode. For example, mechanical balance for a new AMB rotor system may meet the operating requirements, it does not require to suppress synchronous vibration in the early stage. But due to corrosion, cracks or residues, etc., which may lead to the rotor mass imbalance become serious. In this case, it is necessary to active the vibration control to avoid system performance degradation, loss reduction and safety risks.

In order to meet the requirements stated above, this paper proposed a parallel control scheme to realize the plug-in mode in the basis of the existing AMB control system. This control scheme can provide convenient control means for the AMB system, as shown in Fig.4.

Here, several main reasons for the parallel plug-in control scheme design are explained below:

Firstly, the existing AMB control system can be used to maintain the stability of the system, and can suppress the non-periodic vibrations. So the parallel control scheme can make up for the deficiency of ILC on non-periodic disturbance control.

Secondly, the structure shown in Fig.4 facilitates to process and analyze the system control error $e_k(t)$. Because the synchronous vibration signal $\tilde{e_k}(t)$ is need to be extracted and calculated at the end of each iteration, and then stored and used as the control error for ILC loop in the next iteration.

Thirdly, the parallel plug-in control scheme can reduce the cost of controller redesign as there is no need to change the existing AMB control system, and can be used to optimize the performance of the AMB system. From another point of view, the parallel control scheme shown in Fig.4 has important practical significance in the application.

C. ALGORITHM CONTROL ANALYSIS

As the analysis of Section II, the reasons why ILC can be used for the AMB rotor synchronous vibration is that, the vibration generated by unbalance force has the same or multi-frequency with ω.

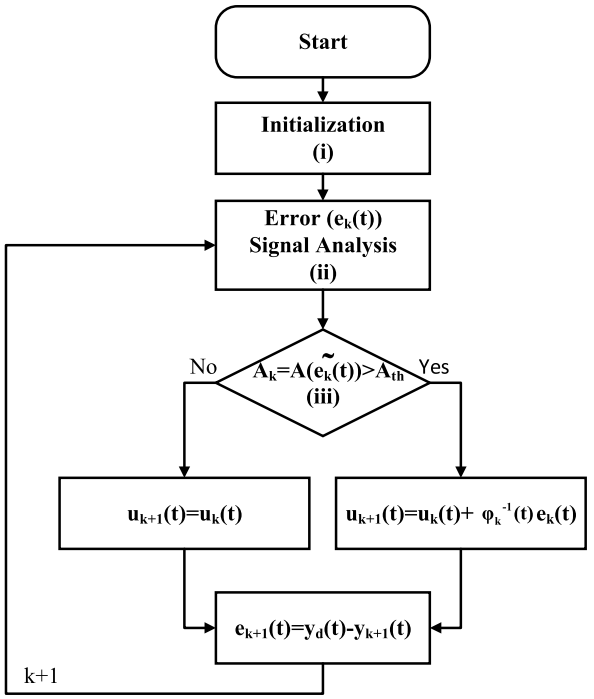

FIGURE 5. Control flow of the algorithm.

Therefore, in order to achieve repeatability and periodicity of the vibration produced by unbalance force, the period of one spin should be used as the iterative learning period T. So the information of the rotor rotational speed is detected real-time, and used to trigger each iteration of ILC. This function can be achieved by the speed sensor mounted on the side of the rotor (as shown in Fig.2). Meanwhile, the ILC controller is developed on the basis of TMS320F28335 and its embedded platform. The main control flow of the algorithm is shown in Fig.5.

There are several key processes described as follows:

(i) Parameters initialization. The ILC parameters are initialized according to Section III.

(ii) The system control error signal analysis. The synchronous vibration signal should be extracted and stored at the end of each iteration. The extraction

algorithm can be performed according to the principle of the discrete Fourier transform (DFT) [49]. Here, the extraction processes of the synchronous vibration are described as follows:

The first step is to calculate the coefficients of the synchronous component according to equation (20).

$$\begin{cases} a_{1k} = \sum_{i=0}^{N-1} e_k[i]\cos(\frac{2\pi i}{N}) \\ b_{1k} = \sum_{i=0}^{N-1} e_k[i]\sin(\frac{2\pi i}{N}) \end{cases} \tag{20}$$

The second step is to synthesize synchronous vibrations$\tilde{e_k}[i]$ by using the inverse discrete Fourier transform (IDFT) [49]. The process can be expressed as

$$\tilde{e_k}[i]\,|_{i=0}^{\frac{N-1}{}} = \frac{2}{N}\left(a_{1k}\cos\left(\frac{2\pi i}{N}\right) + b_{1k}\sin\left(\frac{2\pi i}{N}\right)\right) \tag{21}$$

$$\tilde{e_k}[i]\,|_{i=0}^{\frac{N-1}{}} = A_{1k}\cos(\frac{2\pi i}{N} - \theta) \tag{22}$$

$$\begin{cases} A_{1k} = \frac{2}{N}\sqrt{a_{1k}^2 + b_{1k}^2} \\ tan\theta = \frac{b_{1k}}{a_{1k}} \end{cases} \tag{23}$$

where N is the number of sampling numbers in each spin, and here the iterative learning length meets

$$T =^{\Delta} N, \left(T = \frac{N}{f_s}\right) \tag{24}$$

where f_s is sampling frequency. Obviously, this is consistent with the ILC algorithm described in Section III.

(iii) Trigger ILC loop. As the strategy of ''on demand'' is used in the AMB rotor synchronous vibration. Here we specify that, the ILC loop is active when the vibration amplitude exceeds a certain threshold, and the trigger threshold A_{th} is set to 1/5 of the catcher bearing radius.

V. EXPERIMENTAL RESEARCH

A. SIMULATION RESEARCH

In order to provide a better experimental reference before the experiments, it is necessary to carry out the simulation researches.

In this paper, simulation researches are carried out by using the parameters of the AMB experimental system shown in Fig.2, which are listed in Table 1.

In the simulations, a sinusoidal disturbance with period $T = 10$s and a random white noise are added into the loop in front of power amplifier. Here the sinusoidal disturbance is used to simulate the synchronous vibration caused by the rotor mass imbalance, and the random white noise is used to simulate the random noise in the field. Then, we set $k = 10, x_k(0) = 0$ and $A_{th} = 0$ as the iterations is set to 10, which means that the strategy of ''on demand'' is not used

TABLE 1. Parameters of the AMB experimental system.

Parameter	Value
m	62kg
k_i	145N/A
k_x	62500N/m
f_s	1×10^4Hz

TABLE 2. Parameters of simulations.

Simulation Groups	λ	$\varphi_0(t)$	$[\frac{\partial \mathcal{H}(u_k(t))}{\partial u_k(t)}]^{-1}$	Simulation Results
Group 1	1	1	1	Fig.6
Group 2	1	10	0.1	Fig.7
Group 3	10	10	0.1	Fig.8
Group 4	1	0.1	10	Fig.9

in simulations. Four groups of simulations are carried out with the parameters initialed as shown in Table 2. Furthermore, we select the curves of the vibration signal both in the iterative domain and time domain, the maximum vibration amplitude and the10th P-D as references for the comparative analysis in four simulations.

The results of four simulations are analyzed as follows:

Firstly, the results of Group 1, Group 2 and Group 3 reveal that the MFC method can effectively suppress synchronous vibration.

Secondary, comparing Group 1 and Group 2, in the case with the same value of λ, but different values of $\varphi_0(t)$, it reveals that $\varphi_0(t)$ can affect the system control error convergence speed. Meanwhile, the larger the $\varphi_0(t)$, the smaller the $[\frac{\partial \mathcal{H}(u_k(t))}{\partial u_k(t)}]^{-1}$, which means that the iterative learning gain is smaller, and the system control error convergence speed is slower.

Third, comparing Group 2 and Group 3, in the case with the same value of $\varphi_0(t)$, but different values o fλ, it reveals that λ hardly affect the system control error convergence speed. This experimental result is consistent with that λ does not affect the optimal value of equation (15).

Finally, from the calculation results of $\varphi_{10}(t)$ in Group 1, Group2 and Group 3, all $\varphi_{10}(t) > 0.1$ and $\frac{1}{\beta} < 10$. But in Group 4, we set $\varphi_0(t) = 0.1$, this means $[\frac{\partial \mathcal{H}(u_k(t))}{\partial u_k(t)}]^{-1} = 10$, where the iterative learning gain exceeds the system control error convergence range, and eventually leads to the system control error divergence. So $\varphi_0(t)$ is a sensitive parameter in the MFC for the AMB rotor synchronous vibration.

B. EXPERIMENTAL RESEARCH

The simulation results can provide references for the experimental researches. For example, we know how to select λ

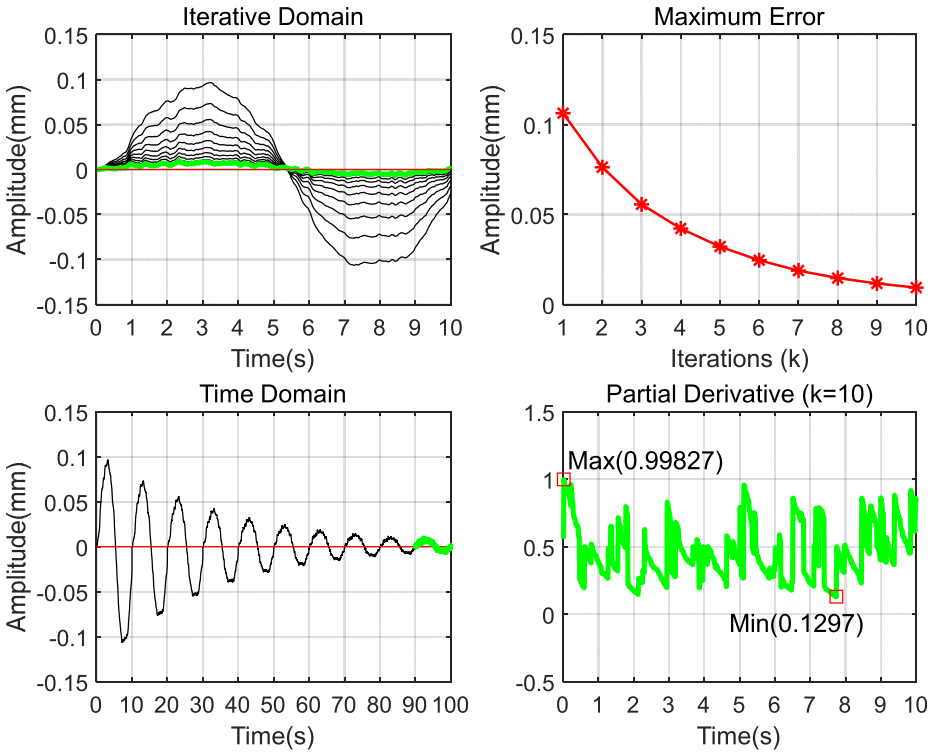

FIGURE 6. Simulation results of Group 1 ($\lambda = 1, \varphi_0(t) = 1$).

and $\varphi_0(t)$, and the influence of λ on the control effect is almost negligible. So here we set $\lambda = 1$ in all experiments. Considering that the identical initial conditions cannot be fully met in the AMB experimental system for synchronous vibration with ILC, which means the initial states of the system described in equation (6) would varied in each cycle (iteration), or more direct to say that $x_k(0) = x_0$ would not be satisfied. Therefore, here we apply a forgetting factor to realize the robustness of the ILC with reference to [36], [37]. Finally, the algorithm used in the experiments is revised as

$$u_{k+1}(t) = \xi_{ff} u_k(t) + [\frac{\partial \mathcal{H}(u_k(t))}{\partial u_k(t)}]^{-1} e_k(t) \qquad (25)$$

where $\xi_{ff} \epsilon [0, 1)$, the role of ξ_{ff} is to gradually weaken the use of the previous system information as the iteration progresses.

And it is an engineering experience parameter, so $\xi_{ff} = 0.95$ is set in the experiments. Here, the experiments are carried out at the $f = 25$Hz (the speed of rotor is 1500 r/m), because synchronous vibration is very serious as the converter operates in this frequency.

Four groups of experiments are carried out with the parameters shown in Table 3. And we select the time-domain vibration signal of one direction and its P-D calculated in the 20th iteration. Meanwhile, we draw the rotor's axis loci of the places where is installed displacement sensors with and without the ILC.

The first 20 iterations are selected for comparative analysis of four experiments. Now the results are analyzed as follows:

TABLE 3. Parameters of experiments.

Experimental Groups	λ	$\varphi_0(t)$	$[\frac{\partial \mathcal{H}(u_k(t))}{\partial u_k(t)}]^{-1}$	A_{th} (mm)	Experimental Results
Group 5	1	1	1	0.03	Fig.10
Group 6	1	10	0.1	0.03	Fig.11
Group 7	1	1	1	0	Fig.12
Group 8	1	10	0.1	0	Fig.13

Note 1. The safety space between the surface of rotor and catcher bearing is 0.15mm in the AMB experimental system

Firstly, the experimental results (shown in Fig.10, Fig.11, Fig.12 and Fig.13) reveal that the MFC method can effectively suppress AMB rotor vibration.

Secondary, from the results of Group 5 and Group 6 with the threshold control strategy, we can see that $\varphi_0(t)$ can affect the system control error convergence speed. The control requirement is met after the 12th iteration in Group 5 and after the 14th iteration in Group 6. Of course the system control error convergence speed can also be revealed in Group 7 and Group 8 without the threshold control strategy.

Third, the 20th P-D calculation results of four experiments are basically consistent and coincided with the simulation results, which indicate that the P-D calculated in the AMB experimental system are accurate and reliable. So it is reasonable and feasible to be used as a reference to adjust the ILC gain.

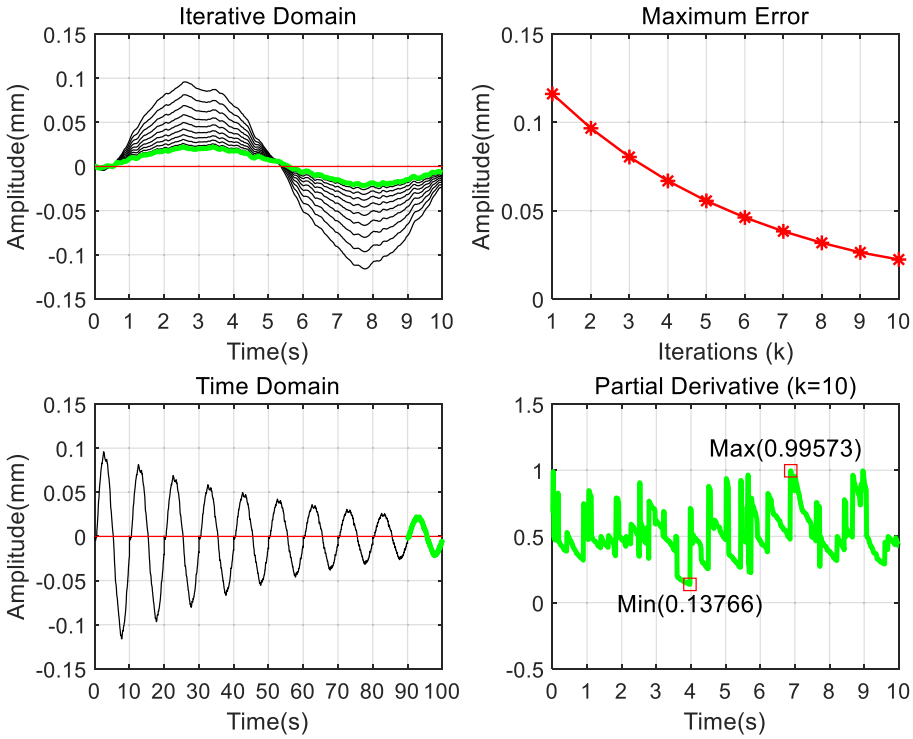

FIGURE 7. Simulation results of Group 2 ($\lambda = 1, \varphi_0(t) = 10$).

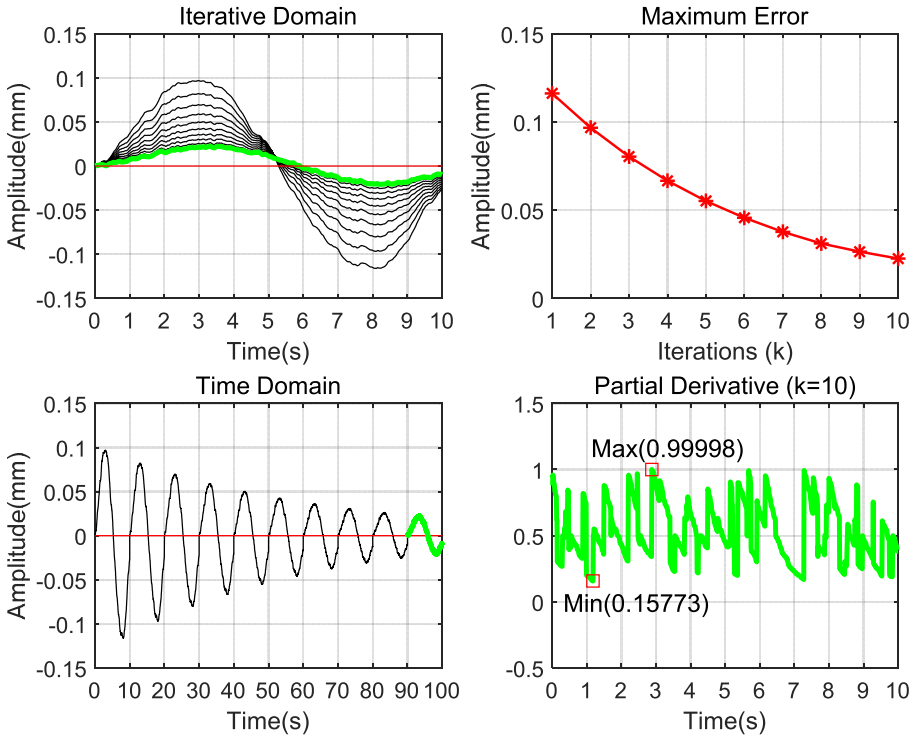

FIGURE 8. Simulation results of Group 3 ($\lambda = 10, \varphi_0(t) = 10$).

Finally, we can see the amplitude and the rotor's axis loci have changed with and without ILC. From the results of Group 5 and Group 6 with the threshold control strategy, when the control requirements are met, the remaining vibration signals still have certain periodic characteristics, because the rotor's axis loci are small circulars or ovals (shown in Fig.10 and Fig.11). However, from the results of Group 7 and Group 8 without the threshold control strategy,

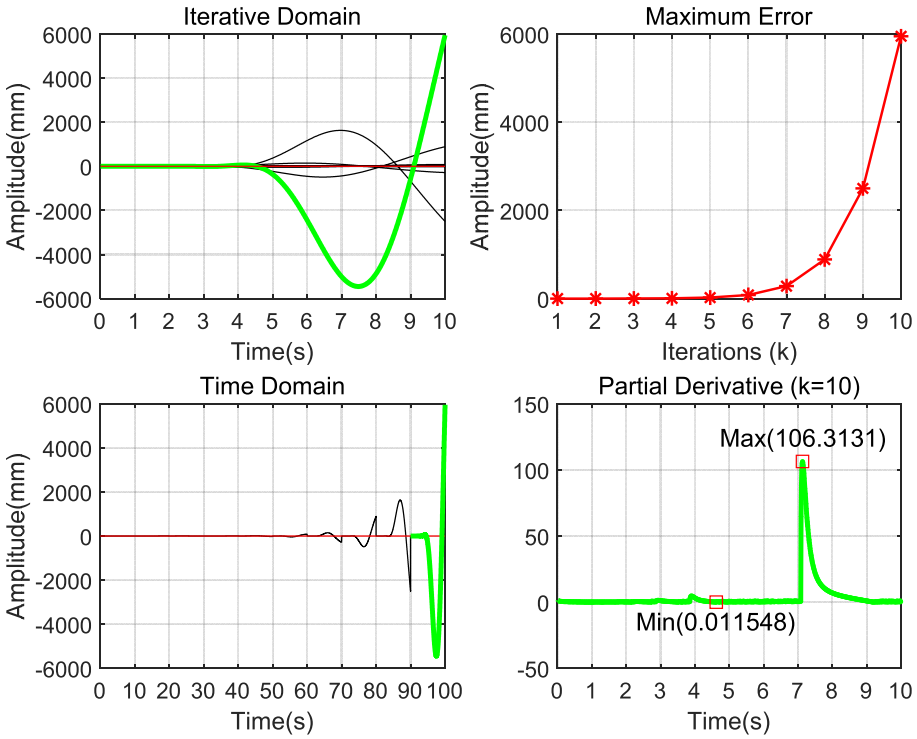

FIGURE 9. Simulation results of Group 4 ($\lambda = 1, \varphi_0(t) = 0.1$).

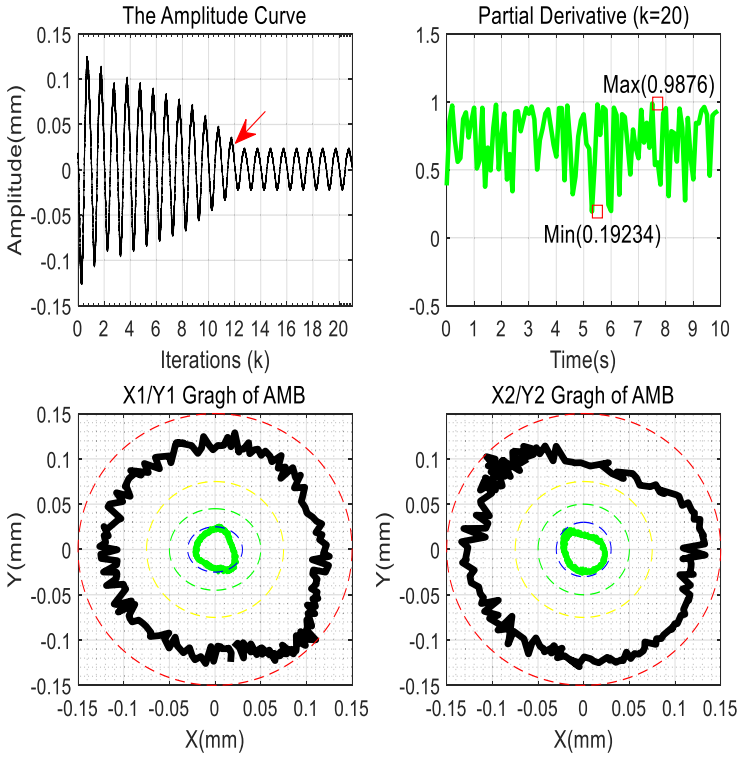

FIGURE 10. Experimental results of Group 5 ($\lambda = 1, \varphi_0(t) = 1, A_{th} = 0.03$).

the control requirement is met after the 15th iteration in Group 7 and after the 17th iteration in Group 8, and there are almost no periodic components in the remaining vibration signals, because the rotor's axis loci converge into small clusters (shown in Fig.12 and Fig.13).

C. RESULTS DICUSSION

From the results of simulations and experiments, the MFC method designed in this paper has a good control effect on the AMB rotor synchronous vibration. The key of the algorithm is to set the initial values of two parameters

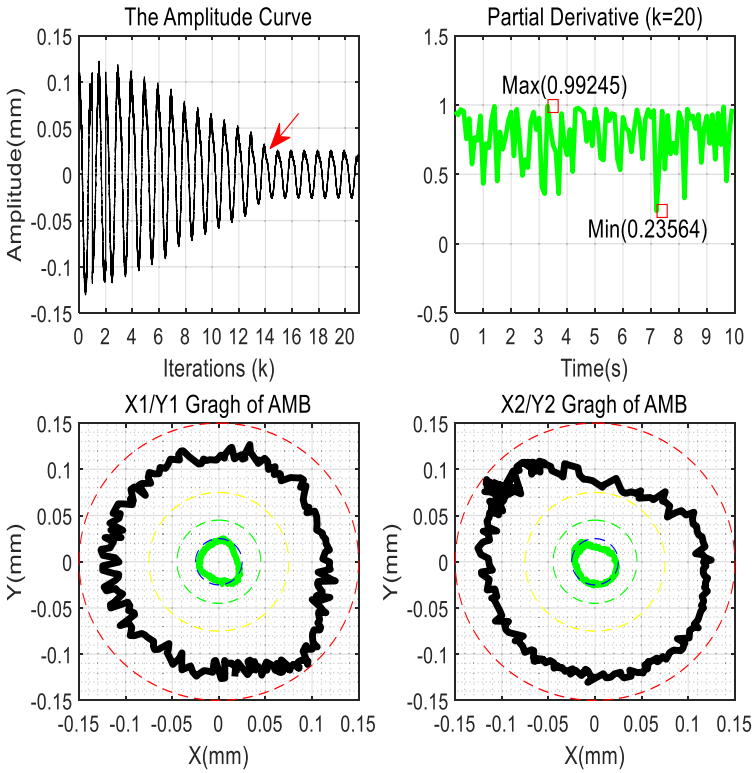

FIGURE 11. Experimental results of Group 6 ($\lambda = 1, \varphi_0(t) = 10, A_{th} = 0.03$).

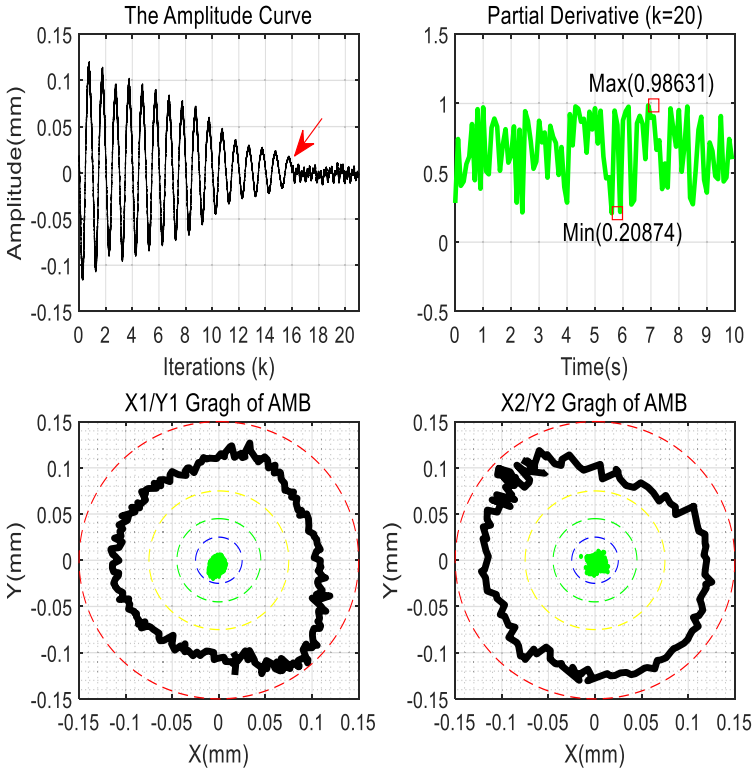

FIGURE 12. Experimental results of Group 7 ($\lambda = 1, \varphi_0(t) = 1, A_{th} = 0$).

λ and $\varphi_0(t)$. Firstly, the control factor λ is insensitive to the control effect, so a reasonable positive number is only needed to be selected appropriately. Secondary, the selection of $\varphi_0(t)$ is very critical. From the experimental results, it is better to set the value of $\varphi_0(t)$ to be large, which means the expected P-D is large. Thus, the initial iteration learning gain is small, so it

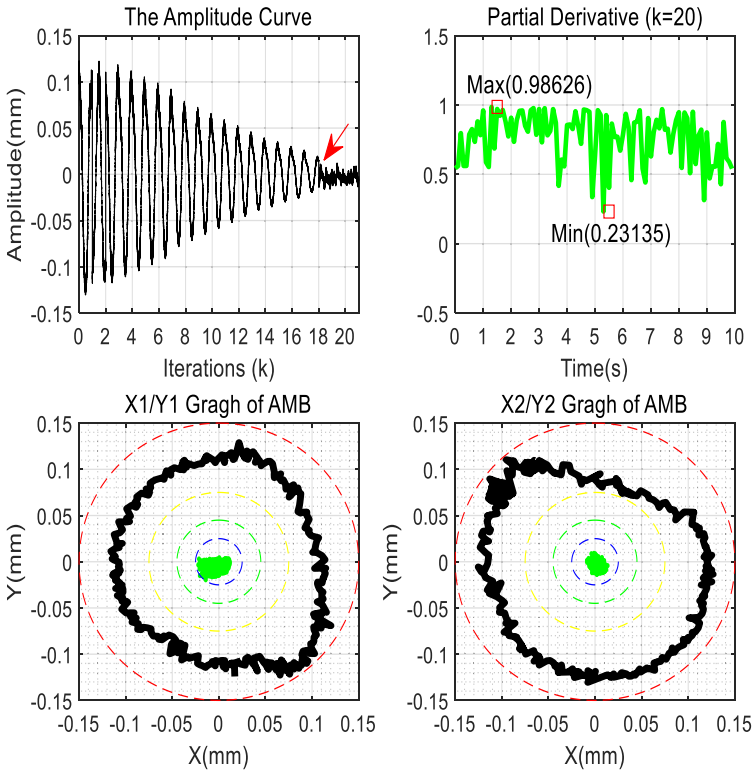

FIGURE 13. Experimental results of Group 8 ($\lambda = 1, \varphi_0(t) = 10, A_{th} = 0$).

does not affect the system convergence, but would sacrifice convergence speed of the system control error. Of course, this is allowed in vibration control. On the contrary, if the expected P-D is small, the initial iterative learning gain will be large, which would lead to the system instability.

From the above analysis, four parameters (ξ_{ff}, A_{th}, λ and $\varphi_0(t)$) are needed to set before experiments, and the model of AMB is unknown in the ILC loop. Of course, if the system model is known, the parameters will be set more direct and effective, and the synchronous vibration will be suppressed rapidly. But if the system model is unknown, or the model is dynamically changed, the parameters can be conservatively initialized and the ILC loop can learn by using the previous system information until the control requirements are met. However, an accurate mathematical model of plant is difficult to be obtained, especially for the AMB with strong nonlinear and strong coupling stated in this paper. In reality, the vibration index meets the requirements of many AMB system, but the vibration performance would be deteriorated as the system structures are varied in the operation process. It can be seen that it is not realistic to build the model of a dynamic AMB system. So the MFC studied in this paper is very attractive to suppress synchronous vibration of the AMB system.

In summary, the MFC method based on Newton-type ILC proposed in this paper and its application in AMB synchronous vibration have many characteristics described as follows:

(1) The P-D introduced in this paper is used to solve the shortcomings of the traditional SISO ILC algorithms based on Newton method. The experimental results prove the MFC is suitable for the AMB rotor synchronous vibration control.

(2) The MFC proposed in this paper is simple in principle, and can fully achieved the online self-learning function. Meanwhile, this algorithm reduces the burden of online computation, which can meet the real-time requirement for the AMB control system.

(3) The control scheme proposed in this paper is practical, and the algorithm does not need any plant model, and the control method can be used as an effective means to optimize and upgrade the AMB system.

VI. CONCLUSION

As one of the most promising bearing, AMB has many incomparable advantages that traditional bearings cannot match. However, complicated unbalance problems block the future application and development of AMB. In this paper, the MFC method designed can effectively achieve the AMB rotor synchronous vibration control, without using the complex and varied system model.

At the same time, with the help of variable length in ILC algorithm, it is easy to realize the rotor unbalance control at variable speed, which is not involved in the paper, but it has been implemented in the AMB experimental system. Furthermore, we will continue to research the multivariable

MFC method based on Newton-type ILC algorithm because there exists five DOFs in AMB, and the impact of abnormal data in ILC loop because the vibration control would be applied in the digital control system. And our future woks are focused on, but not limited in, the following aspects:

(1) How to achieve the AMB rotor synchronous vibration control under the strong coupling of four DOFs in the radial directions.
(2) How to suppress the multi-frequency vibrations caused by the sensor runout and the unbalance magnetic pull produced by the misalignment of the geometric center between the stator and the rotor, or the circuit imbalance in the motor converter, AMB power amplifier or pole winding, etc.
(3) How to apply the synchronous vibration control method proposed in this paper to primary helium circulator in high temperature gas cooled reactor.

REFERENCES

[1] G. Schweitzer and E. H. Maslen, Eds., *Magnetic Bearings: Theory, Design, and Application to Rotating Machinery*. Berlin, Germany: Springer, 2009. [Online]. Available: https://link.springer.com/
[2] G. Yang, Z. Shi, and N. Mo, "Technical design and engineering prototype experiment of active magnetic bearing for helium blower of HTR-PM," *Ann. Nucl. Energy*, vol. 71, no. 9, pp. 103–110, Sep. 2014.
[3] Y. Zheng, Z. Shi, and X. Liu, "Design and Analysis of electromagnetic bearing safety control system for HTGR primary helium circulator," presented at the 26th Int. Conf. Nucl. Eng. (ICONE26). London, U.K.: ASME, Jul. 2018.
[4] Y. Le, J. Sun, and B. Han, "Modeling and design of 3-DOF magnetic bearing for high-speed motor including eddy-current effects and leakage effects," *IEEE Trans. Ind. Electron.*, vol. 63, no. 6, pp. 3656–3665, Jun. 2016.
[5] J. K. Sinha, Eds., "Vibration engineering and technology of machinery," in *Proc. VETOMAC-X*, Manchester, U.K., Sep. 2014, pp. 939–949. [Online]. Available: https://link.springer.com/
[6] J. Fang, X. Xu, and J. Xie, "Active vibration control of rotor imbalance in active magnetic bearing systems," *J. Vib. Control*, vol. 21, no. 4, pp. 684–700, Mar. 2015.
[7] J. Zhou, S. Zheng, B. Han, and J. Fang, "Effects of notch filters on imbalance rejection with heteropolar and homopolar magnetic bearings in a 30-kW 60 000-r/min motor," *IEEE Trans. Ind. Electron.*, vol. 64, no. 10, pp. 8033–8041, Oct. 2017.
[8] Q. Chen, G. Liu, and B. Han, "Suppression of imbalance vibration in AMB-rotor systems using adaptive frequency estimator," *IEEE Trans. Ind. Electron.*, vol. 62, no. 12, pp. 7696–7705, Dec. 2015.
[9] H. Wang, P. X. Liu, X. Xie, X. Liu, T. Hayat, and F. E. Alsaadi, "Adaptive fuzzy asymptotical tracking control of nonlinear systems with unmodeled dynamics and quantized actuator," *Inf. Sci.*, Apr. 2018.
[10] H. Wang, P. X. Liu, X. Zhao, and X. Liu, "Adaptive fuzzy finite-time control of nonlinear systems with actuator faults," *IEEE Trans. Cybern.*, to be published.
[11] Z. Lyu, Z. Liu, Y. Zhang, and C. L. P. Chen, "Adaptive neural control for switched nonlinear systems with unmodeled dynamics and unknown output hysteresis," *Neurocomputing*, vol. 341, pp. 107–117, May 2019.
[12] J.-K. Huusom, N.-K. Poulsen, and S.-B. Jørgensen, "Iterative feedback tuning of uncertain state space systems," *Brazilian J. Chem. Eng.*, vol. 27, no. 3, pp. 461–472, Sep. 2010.
[13] R.-E. Precup, M.-B. Rădac, M.-L. Tomescu, E. M. Petriu, and S. Preitl, "Stable and convergent iterative feedback tuning of fuzzy controllers for discrete-time SISO systems," *Expert Syst. Appl.*, vol. 40, no. 1, pp. 188–199, Jan. 2013.
[14] I. Arredondo and J. Jugo, "2-DOF controller design for precise positioning a spindle levitated with active magnetic bearings," *Eur. J. Control*, vol. 18, no. 2, pp. 194–206, 2012.
[15] S.-L. Chen, "Nonlinear smooth feedback control of a three-pole active magnetic bearing system," *IEEE Trans. Control Syst. Technol.*, vol. 19, no. 3, pp. 615–621, May 2011.
[16] H. M. N. K. Balini, J. Witte, and C. W. Scherer, "Synthesis and implementation of gain-scheduling and LPV controllers for an AMB system," *Automatica*, vol. 48, no. 3, pp. 521–527, Mar. 2012.
[17] G. Schweitzer. (1985). *Magnetic Bearings for Vibration Control*. [Online]. Available: http://community.ebooklibrary.org/
[18] K. Zhang and X.-Z. Zhang, "A review of unbalance control technology of active magnetic bearings," *China Mech. Eng.*, vol. 21, no. 8, pp. 897–903, Apr. 2010.
[19] P.-C. Tung, M.-T. Tsai, K.-Y. Chen, Y.-H. Fan, and F.-C. Chou, "Design of model-based unbalance compensator with fuzzy gain tuning mechanism for an active magnetic bearing system," *Expert Syst. Appl.*, vol. 38, no. 10, pp. 12861–12868, Sep. 2011.
[20] S. Okubo, Y. Nakamura, and S. Wakui, "A design method of a mode control and an unbalance vibration control for five-axes active magnetic bearing systems," *Int. J. Adv. Mech. Syst.*, vol. 5, no. 4, pp. 257–269, 2013.
[21] C. Kang and T.-C. Tsao, "Control of magnetic bearings for rotor unbalance with plug-in time-varying resonators," *J. Dyn. Syst. Meas., Control*, vol. 138, no. 1, Oct. 2015, Art. no. 010111.
[22] C. Bi, D. Wu, Q. Jiang, and Z. Liu, "Automatic learning control for unbalance compensation in active magnetic bearings," *IEEE Trans. Magn.*, vol. 41, no. 7, pp. 2270–2280, Jul. 2005.
[23] Y. He, "Research on unbalance control for multi-variable active magnetic bearing system," Ph.D. dissertation, INET, Tsinghua Univ., Beijing, China, 2017.
[24] J.-X. Xu, S.-K. Panda, and T.-H. Lee, *Real-time Iterative Learning Control: Design and Applications*. London, U.K.: Springer, 2009.
[25] W. He, T. Meng, D. Huang, and X. Li, "Adaptive boundary iterative learning control for an Euler–Bernoulli beam system with input constraint," *IEEE Trans. Neural Netw. Learn. Syst.*, vol. 29, no. 5, pp. 1539–1549, May 2018.
[26] W. He, T. Meng, X. He, and S. S. Ge, "Unified iterative learning control for flexible structures with input constraints," *Automatica*, vol. 96, pp. 326–336, Oct. 2018.
[27] D. Shen, *Iterative Learning Control with Passive Incomplete Information: Algorithms Design and Convergence Analysis*. London, U.K.: Springer, 2018.
[28] D. Shen and J.-X. Xu, "A novel Markov chain based ILC analysis for linear stochastic systems under general data dropouts environments," *IEEE Trans. Autom. Control*, vol. 62, no. 11, pp. 5850–5857, Nov. 2017.
[29] X. Bu, Z. Hou, S. Jin, and R. Chi, "An iterative learning control design approach for networked control systems with data dropouts," *Int. J. Robust Nonlinear Control*, vol. 26, no. 1, pp. 91–109, Jan. 2016.
[30] F. Song, Y. Liu, J.-X. Xu, X. Yang, P. He, and Z. Yang, "Iterative learning identification and compensation of space-periodic disturbance in PMLSM systems with time delay," *IEEE Trans. Ind. Electron.*, vol. 65, no. 9, pp. 7579–7589, Sep. 2018.
[31] D. A. Bristow, "Iterative learning control for precision motion control of microscale and nanoscale tracking systems," Ph.D. dissertation, Mech. Eng. Graduate College, Univ. Illinois Urbana-Champaign, Champaign, IL, USA, May 2007.
[32] C. Peng and Q. Zhou, "Direct vibration force suppression for magnetically suspended motor based on synchronous rotating frame transformation," *IEEE Access*, vol. 7, pp. 37639–37649, 2019.
[33] L. Christian, *Mechanical Vibration and Shock Analysis: Sinusoidal Vibration*, 3rd ed. London, U.K.: Wiley, 2014.
[34] C. Di, I. Petrov, J. J. Pyrhönen, and X. Bao, "Unbalanced magnetic pull compensation with active magnetic bearings in a 2 MW high-speed induction machine by FEM," *IEEE Trans. Magn.*, vol. 54, no. 8, Aug. 2018, Art. no. 8202913.
[35] S. Arimoto, S. Kawamura, and F. Miyazaki, "Bettering operation of robots by learning," *J. Robot. Syst.*, vol. 1, no. 2, pp. 123–140, 1984.
[36] J.-X. Xu and Y. Tan, *Linear and Nonlinear Iterative Learning Control*. New York, NY, USA: Springer, 2003. [Online]. Available: https://link.springer.com/
[37] D.-H. Owens, *Iterative Learning Control*. London, U.K.: Springer, 2016. [Online]. Available: https://link.springer.com/
[38] Z. Wang, Z. Song, and Q. Zeng, "A new iterative learning control with time delays for LTI systems in frequency domain," *IEEE Access*, vol. 7, pp. 13355–13363, 2019.
[39] S. Sun, T. Endo, and F. Matsuno, "Iterative learning control based robust distributed algorithm for non-holonomic mobile robots formation," *IEEE Access*, vol. 6, pp. 61904–61917, 2018.

[40] Q. Yan, J. Cai, L. Wu, and Q. Zhou, "Error-tracking iterative learning control for nonlinearly parametric time-delay systems with initial state errors," *IEEE Access*, vol. 6, pp. 12167–12174, Jan. 2018.
[41] T. Ngo, M. H. Nguyen, Y. Wang, J. Ge, S. Wei, and T. L. Mai, "An adaptive iterative learning control for robot manipulator in task space," *Int. J. Comput. Commun. Control*, vol. 7, no. 3, pp. 518–529, Sep. 2012.
[42] T. Lin, D. H. Owens, and J. Hätönen, "Newton method based iterative learning control for discrete non-linear systems," *Int. J. Control*, vol. 79, no. 10, pp. 1263–1276, 2006.
[43] T. Lin, D. H. Owens, and J. Hatonen, "Newton-method based iterative learning control for sampled nonlinear systems," in *Proc. 4th Int. Workshop Multidimensional Syst.*, 2005, pp. 142–147.
[44] W. Xiao, D. Cong, and Z. Yang, "Modified Quasi–Newton optimization algorithm-based iterative learning control for multi-axial road durability test rig," *IEEE Access*, vol. 7, pp. 31286–31296, 2019.
[45] G. Xu, C. Shao, and Y. Han, "Iterative learning control based on quasi-Newton methods," *J. Supercomput.*, vol. 67, no. 3, pp. 653–670, Mar. 2014.
[46] S. G. Sankaran and A. A. L. Beex, "Convergence behavior of affine projection algorithms," *IEEE Trans. Signal Process.*, vol. 48, no. 4, pp. 1086–1096, Apr. 2000.
[47] Z. Hou, R. Chi, and H. Gao, "An overview of dynamic-linearization-based data-driven control and applications," *IEEE Trans. Ind. Electron.*, vol. 64, no. 5, pp. 4076–4090, May 2017.
[48] Z. S. Hou and S. T. Jin, *Model Free Adaptive Control: Theory and Applications*. Boca Raton, FL, USA: CRC Press, 2013.
[49] D. Sundararajan, *The Discrete Fourier Transform: Theory, Algorithms and Applications*. Singapore: World Scientific, 2001.

YANGBO ZHENG received the B.S. degree in automation from North China Electric Power University (NCEPU), China, in 2007, and the M.S. degree in the Shenyang Institute of Automation, Chinese Academy of Sciences (SIA, CAS), China, in 2010. And he is currently pursuing the Ph.D. degree in the Institute of Nuclear and New Energy Technology (INET), Tsinghua University, China. His research interest includes active magnetic bearing control technology.

NI MO was born in Hunan, China, in 1982. He received the M.S. and Ph.D. degrees in electrical engineering (EEA), Tsinghua University, China, in 2004 and 2009, respectively. He is currently an Associate Researcher in the Institute of Nuclear and New Energy Technology (INET), Tsinghua University. His research interests include control applications and electrical designing in optimization of magnetic bearing systems.

YAN ZHOU received the B.S. and M.S. degrees in automation from Beihang University, China, in 2002 and 2005, respectively. She is currently working at the Institute of Nuclear and New Energy Technology (INET), Tsinghua University. Her research interests include AMB amplifiers and control systems and its applications.

ZHENGANG SHI received the B.S. degree in engineering physics, Tsinghua University, China, in 1997, the M.S. and Ph.D. degrees in the Institute of Nuclear and New Energy Technology (INET), Tsinghua University, China, in 2000 and 2003, respectively. He is working as the Head of magnetic bearing laboratory. His research interests include magnetic bearing technology and nuclear power generation technology.